Journal of Innovations in Engineering Education
JIEE 2026, Vol. 9, Issue 1.

https://doi.org/10.3126/jiee.v9i1.90526

THAPATHALI CAMPUS
Institute of Engineering
Tribhuvan University

Analytical and FEA-based evaluation of natural frequencies of aircraft power turbine blades for resonance zone identification and comparative material suitability assessment

Jivan Pokhrel[a], Kamal Pokharel [a,*] and Rajiv Kumar Khadka [a]

[a]*Department of Automobile and Mechanical Engineering, Thapathali Campus, Institute of Engineering,Tribhuvan University, Thapathali, Kathmandu, Nepal*

ARTICLE INFO

Article history:

Received 3 February 2026
Revised in 16 February 2026
Accepted 1 April 2026

Keywords:

Natural frequency
Power turbine blade
Centrifugal stiffening
Campbell diagram
Material selection

Abstract

Natural frequencies strongly influence the vibration response of aircraft power turbine blades operating at high rotational speeds and elevated temperatures. Resonance under such conditions can lead to excessive vibration, fatigue damage, and blade failure. In this study, the natural frequencies of a power turbine blade are evaluated using an analytical beam-based approach that includes centrifugal stiffening and temperature-dependent material properties. The analytical results are validated through finite element modal analysis. Three materials Titanium Alloys - Ti6Al4V, Inconel-738, and CM-247 LC are examined at an operating temperature of 850 °C and rotational speeds up to 32,000 rpm. The comparison shows good agreement between analytical and numerical results. The study highlights the influence of material stiffness degradation at high temperature and demonstrates that CM-247 LC offers the most stable vibrational performance under combined thermal and rotational loading.

1. Introduction

Power turbine blades in aircraft gas-turbine engines operate under severe thermal and mechanical conditions, including high rotational speeds and temperatures. These conditions significantly affect the vibration behavior of the blades and increase the risk of resonance when excitation frequencies coincide with natural frequencies. Resonance-induced vibration is a major cause of fatigue damage in turbine blades, therefore the accurate prediction of natural frequencies is essential for safe and reliable design. The natural frequencies of turbine blades depend on material properties, blade geometry, temperature, and rotational speed. While centrifugal forces increase structural stiffness during rotation, elevated temperatures reduce material stiffness, resulting in complex dynamic behavior. Therefore, vibration analysis that accounts for both rotational and thermal effects provides a more realistic assessment than simplified room-temperature analyses. This study focuses on evaluating and validating the natural frequencies of a power turbine blade under realistic operating conditions and assessing material suitability for high-temperature, high-speed applications.

Figure 1, shows the basic internal structure of a turboshaft engine with its main components in a pictorial form.

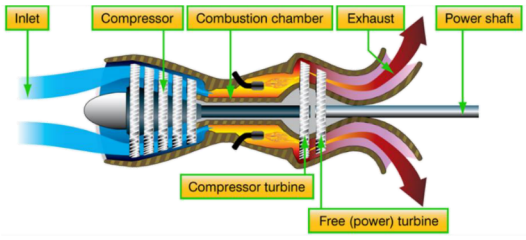

Figure 1: Turbo engine structure [1]

1.1. Objectives of the study

- To develop an approximate analytical model for estimating the natural frequencies of an aircraft power turbine blade.

*Corresponding author:
kpokharel@tcioe.edu.np (K.P.)

- To evaluate blade natural frequencies under non-operating(static) and operating (including centrifugal stiffening effects) conditions using the analytical formulation.
- To perform finite element modal analysis in ANSYS to obtain more realistic natural frequencies and mode shapes.
- To compare analytical predictions with finite element results for the first three bending modes.
- To construct Campbell diagrams for each selected material and identify resonance-sensitive frequency regions. material using Campbell diagrams.
- To compare the dynamic performance of three selected materials and assess their suitability based on frequency response, and resonance characteristics.

1.2. Assumptions and limitations of the study

- Natural frequencies are evaluated to the first three bending modes of vibration only while other higher modes are assumed to follow the same trend and are therefore considered beyond the scope of this research.
- Blade geometry and boundary conditions are adopted from published literature rather than a specific aircraft design.
- The blade is idealized as a cantilever beam with uniform rectangular geometry for analytical modeling and materials are assumed to be linear elastic and homogeneous.
- Experimental validation is not included; the study relies on analytical and FEA based comparisons only.

2. Literature review and methods

2.1. Material selection

Materials were chosen based on literature on turbine blade vibration and high-temperature performance. Here Titanium Alloy - Ti6Al4V, Inconel-738, and CM-247 LC were selected due to their common turbine applications and availability of reliable material property data.

All properties in Table 1, taken from published sources [2][3][4], represent the values of different properties of 3 selected materials at room temperature which are used consistently in the whole study for the evaluation of natural frequency of power turbine blade during analytical calculation.

2.2. Design parameters and mechanical restraints

The turbine blade used in this study incorporates a fir-tree root, which is commonly applied in modern turbine designs to ensure secure attachment to the disk and effective load transfer under high thermal and centrifugal conditions [5]. The blade geometry was selected from established turbine design literature. The blade length is 0.108 m, with a chord width of 0.070 m and a uniform thickness of 0.010 m. This results in a thickness-to-chord ratio of approximately 0.14, which is typical of NACA 65-series turbine airfoils [6].

An aspect ratio of 1.55 was adopted to maintain a balance between aerodynamic efficiency and structural stiffness for power turbine stages [7]. Other aerodynamic and geometric parameters were chosen based on standard cascade design practices reported in the literature [8][9][10]. The power turbine blade rotation varies from aircraft to aircraft but it operate at around 20,000 to 25000 rpm and temperature of 800 °C to 900 °C, which are representative of typical aircraft power turbine operating conditions [11][12][13][14]. To check the vibration at operating conditions, natural frequencies are evaluated from 0 to 32,000 RPM and at 850 °C.

2.3. Analytical method

The blade was modeled as a uniform cantilever beam using Euler–Bernoulli beam theory. The first three bending modes were evaluated, including centrifugal stiffening effects. Natural frequencies were calculated at rotational speeds from 0 to 32,000 rpm and at an operating temperature of 850 °C [11][15].

2.4. Numerical method

A three-dimensional blade model based on a NACA 65-series airfoil was developed and analyzed in ANSYS. The root was fixed to represent cantilever conditions, and modal analysis with rotational effects was performed. FEA results for the first three bending modes were used to validate the analytical predictions.

2.5. Resonance assessment

Engine order excitation frequencies were obtained by converting rotational speed from RPM to Hz. The validated natural frequencies were then used to construct Campbell diagrams for each material [16]. These diagrams are analyzed to identify potential resonance zones and to compare the vibrational suitability of the selected materials for power turbine blade applications.

Table 1: Material selection and their properties [2][3][4]

S.N.	Property	Material		
		Ti Alloy- Ti6Al4V	CM-247 LC	Inconel - 738
1	Modulus of elasticity (MPa)	110000	220000	199000
2	Poisson's ratio	0.3	0.3	0.3
3	Density (Kg/m^3)	4429	8530	8150
4	Tensile Strength (MPa)	862	792	1096

2.6. Research gaps and novelity

Previous research on turbine blade dynamics mainly focuses on studying natural frequencies and resonance behavior for individual materials, without comparing different advanced blade alloys under the same thermo-rotational conditions. This creates a clear gap in understanding how different materials with different material properties shift resonance zones and influence safe operating speed ranges. So the novelty of this work lies in its systematic comparison of multiple blade materials using a resonance safety mapping approach, which clearly identifies changes in critical speed locations and resonance-free operating windows. This study directly supports aircraft turbo engine designers by helping them choose the most suitable material for power turbine blades during the design stage.

2.7. Analytical evaluation

The Euler–Bernoulli beam theory is adopted to model the turbine blade, assuming slender geometry with negligible shear deformation and rotary inertia [17][18].

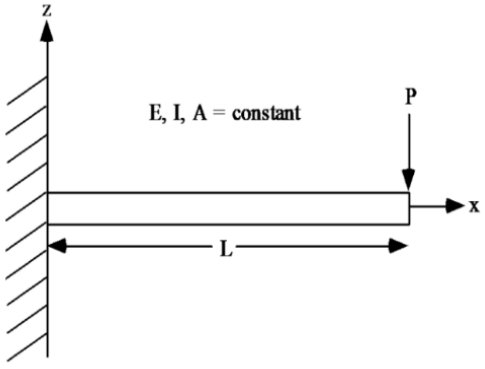

Figure 2: Simple Euler- Bernoulli cantilever beam

The blade is idealized as a uniform cantilever beam, and its free vibration behavior is governed by the following equation:

$$EI\frac{\partial^4 w(x,t)}{\partial x^4} + \rho A\frac{\partial^2 w(x,t)}{\partial t^2} = 0 \tag{1}$$

Equation 1 is the Governing Partial Differential Equation of Beam. The natural frequencies of the beam is calculated using the Equation 2 [19]:

$$\omega_n = \left(\frac{\beta_n^2}{L^2}\right)\sqrt{\frac{EI}{\rho A}} \tag{2}$$

And the first few roots are [20]:

$\beta_1 = 1.8751, \beta_2 = 4.6941, \beta_3 = 7.8548$

Where, E is the elastic modulus and I is the second moment of area of the beam's cross section. ρ, A and L are density, cross-sectional area, and the blade length.

2.8. Effect of temperature

Turbine blades operate at elevated temperatures, which reduce stiffness due to material softening. Incorporating a linear temperature-dependent modulus Equation 3:

$$E_T = E_0\left(1 - \alpha_E \Delta T\right) \tag{3}$$

So the natural frequency at temperature T is given by Equation 4:

$$\omega_{n,T} = \left(\frac{\beta_n^2}{L^2}\right)\sqrt{\frac{E_T I}{\rho A}} \tag{4}$$

Density changes with temperature are negligible in modal analysis.

2.9. Effect of rotation (Centrifugal stiffening)

Centrifugal forces will exist along the span of a rotating blade with high angular speed, these forces will cause an axial tensile load which leads to increase of effective stiffness of blade. This phenomenon is named centrifugal stiffening and it is an important effect in high-speed turbine blades.

Consider a uniform blade rotating with an angular speed Ω, the centrifugal force acting on a differential element is:

$$dF_c = \rho A \Omega^2 x \, dx$$

Integrating along the blade length from root to tip yields the axial centrifugal preload at the root [19]:

$$P_{\text{cent}} = \int_0^L \rho A \Omega^2 x \, dx$$

$$P_{\text{cent}} = \frac{1}{2} \rho A \Omega^2 L^2 \tag{5}$$

When an axial force P from Equation 5 acts on a beam, the governing vibration Equation 5 is modified as Equation 6 [19][20]:

$$EI \frac{\partial^4 w(x,t)}{\partial x^4} + P_{cent} \frac{\partial^2 w(x,t)}{\partial x^2} + \rho A \frac{\partial^2 w(x,t)}{\partial t^2} = 0 \tag{6}$$

Assuming this has linear elastic behavior with small deflections, the transverse displacement is expressed as a harmonic function, Equation 7 [19]:

$$\omega(x,t) = \phi(x) e^{i\omega t} \tag{7}$$

where, $\phi(x)$ describes the mode shape and $e^{i\omega t}$ represents harmonic motion in time.

Double derivative to the Equation 7 gives Equation 8:

$$\frac{\partial^2 w(x,t)}{\partial t^2} = -\omega^2 \phi(x) e^{i\omega t} \tag{8}$$

By substituting Equation 8 in Equation 9, the governing PDE reduces to an ODE, Equation 9 in space.

$$EI \frac{d^4\phi}{dx^4} + P_{cent} \frac{d^2\phi}{dx^2} - \rho A \omega^2 \phi = 0 \tag{9}$$

From vibration theories, let's use a trial function:

$$\phi(x) = e^{kx} \tag{10}$$

This trial step simplifies the spatial derivatives such that the second and fourth derivatives become proportional to the displacement itself, enabling analytical determination of the natural frequencies. To find eigenvalues and actual values of k, it is necessary to take the actual cantilever form;

$$W(x) = C_1 \cos(\beta x) + C_2 \sin(\beta x) + C_3 \cosh(\beta x) + C_4 \sinh(\beta x)$$

For cantilever beam let's have boundaries conditions as: at the root of the beam the displacement and the slope are zero, at the free end of the beam ($x = L$), the moment and shear force are zero. By substituting boundary conditions:

$$\cos(\beta L) \cosh(\beta L) + 1 = 0$$

Solving this transcendental equation for the first few roots yields [20]:

$$(b)_1 = (\beta L)_1 = 1.8751,$$
$$(b)_2 = (\beta L)_2 = 4.6941,$$
$$(b)_3 = (\beta L)_3 = 7.8548.$$

And so, wave number $k = \frac{b_n}{L}$

$$k_1 = \frac{b_1}{L} = \frac{1.8751}{L},$$
$$k_2 = \frac{b_2}{L} = \frac{4.6941}{L},$$
$$k_3 = \frac{b_3}{L} = \frac{7.8548}{L}$$

Then, from Equation 10

$$\frac{d\phi}{dx} = k e^{kx} = k\phi \tag{11}$$

$$\frac{d^2\phi}{dx^2} = k^2 \phi \tag{12}$$

$$\frac{d^4\phi}{dx^4} = k^4 \phi \tag{13}$$

Substitute Equation 11, 12 and 13 into the Equation 9 gives Equation 14,

$$EI \left(k^4 \phi\right) + P_{\text{cent}} \left(k^2 \phi\right) - \rho A \omega^2 \phi = 0$$

$$\omega^2 = \frac{EI}{\rho A} k^4 + \frac{P_{\text{cent}}}{\rho A} k^2 \tag{14}$$

So, for ω_n, $k = \frac{\beta_n}{L}$.

2.10. Combined effect of temperature and rotation

In real conditions, turbine blades experience both high temperature and rotational speed, which affect stiffness in different ways. The corresponding natural frequency f in Hz, combining both effects and substituting P_{cent} is:

$$\frac{1}{2\pi}\sqrt{\beta_n^4 \frac{E_T I}{\rho A L^4}\left(1+\frac{\rho A \Omega^2 L^4}{2E_T I \beta_n^2}\right)} \tag{15}$$

This Equation 15 predicts natural frequencies under simultaneous temperature and rotation, explaining trends in Campbell diagrams.

2.11. Inclusion of damping

Damping minimally affects natural frequencies but influences vibration amplitude. The damped frequency is given by Equation 16:

$$f_d = f_n\sqrt{1-\zeta^2} \tag{16}$$

For turbine blades, $\zeta < 0.02$, so damping is taken negligible in this study [19].

2.12. Natural frequency calculation for Titanium Alloys - Ti6Al4V

The variation of elastic modulus with temperature for Titanium Alloy is obtained from Literature Review [21].

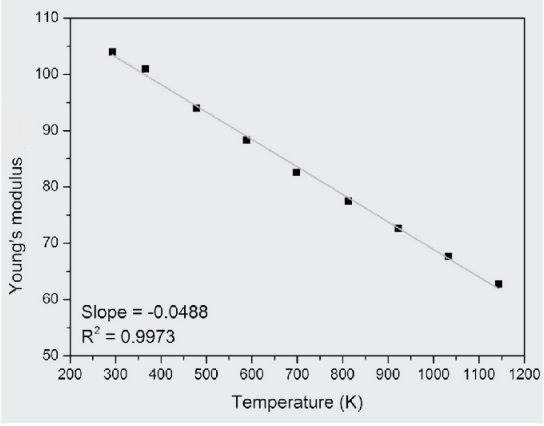

Figure 3: Temperature-dependent Young's modulus for Ti-6Al-4V [21]

Figure 3 is a graph taken from a Literature, which presents experimentally validated values of changes in elastic modulus of Titanium Alloy Ti-6Al-4V with increase in temperature as required in the research.

Based on this literature-supported observation, the Young's modulus at 850 °C is estimated as:

$$E_{850°C} = E_{1123\,K} = 63.3\,\text{GPa} = 63300\,\text{MPa}$$

2.13. Natural frequency calculation for Inconel-738

From the published data for Inconel-738:

Table 2: Elastic modulus variation over small temperature intervals [3]

Temperature (°F)	Young's Modulus, E (Psi)
1400	23.2×10^6
1600	21.9×10^6

Here, Table 2 taken from [3], represents the different values of modulus of elasticity at different temperature. So by interpolating, Elastic Modulus at 850°C is;

$$E_{850°C} = E_{1562°F} = 152703\,\text{MPa}$$

2.14. Natural frequency calculation for CM-247 LC

Within the range of 850 °C, Young's modulus is nearly constant [4]

$$E_{850°C} = E_{RT} = 220000\,\text{MPa}$$

2.15. Mathematical calculation

Here, values of natural frequency for each 3 materials are evaluated and tabulated in Table 3 with 5 different cases which are: Case 1: Natural frequency of power turbine blade made up of each materials at temperature 850 degree Celsius at 0 RPM, Case 2: at 8000 RPM, Case 3: at 16000 RPM, Case 4: at 24000 RPM, and Case 5: at 32000 RPM.

3. FEA modeling

The turbine blade geometry as shown in Figure 4 used in this study was adopted from established literature to ensure a more representative design. To reduce complexity with retaining essential dynamic characteristics, a single blade was modeled with a pre-twisted profile and fir-tree root instead of the full rotor assembly.

The blade model was created in SolidWorks and imported into ANSYS, where it was meshed using a hex-dominant scheme with a refined element size of 1 mm to capture geometric details more closely. Material properties for Ti-6Al-4V, Inconel-738, and CM-247 LC were manually added based on published data, as these advanced alloys are not available in the ANSYS. Therefore, Figure 4 demonstrates the close numerical model

Table 3: Analytical results at 850°C

Material	RPM	Mode	Nat Freq. (Hz)
Titanium Alloy-Ti6Al4V	0	1	523.54
		2	3281.15
		3	9188.24
	8000	1	552.58
		2	3310.87
		3	9218.05
	16000	1	631.73
		2	3398.48
		3	9306.91
	24000	1	745.19
		2	3539.54
		3	9453.17
	32000	1	879.79
		2	3728.26
		3	9653.77
Inconel-738	0	1	599.41
		2	3756.65
		3	10519.78
	8000	1	624.94
		2	3782.67
		3	10545.84
	16000	1	695.91
		2	3859.49
		3	10623.42
	24000	1	800.39
		2	3984.53
		3	10751.81
	32000	1	927.053
		2	4152.75
		3	10928.93
CM-247 LC	0	1	703.26
		2	4407.5
		3	12342.37
	8000	1	725.14
		2	4429.48
		3	12364.56
	16000	1	787.12
		2	4495.43
		3	12430.91
	24000	1	880.901
		2	4603.04
		3	12540.72
	32000	1	997.27
		2	4749.06
		3	12692.85

and used to validate the simplified analytical formulation.

In this analysis, following mode shapes are obtained for initial 3 bending modes of blade as in Figure 5, Figure 6 and Figure 7.

In this analysis, a temperature of approximately 850°C is assumed to represent a moderate operating condition

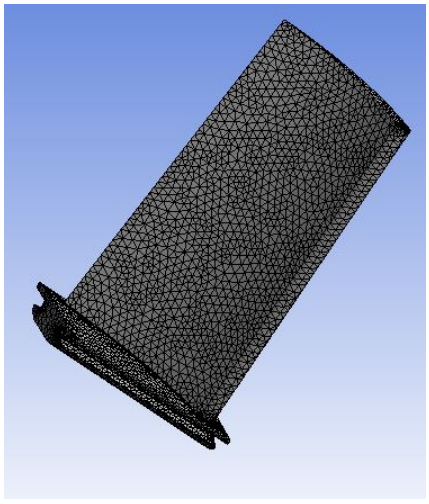

Figure 4: Finite element model of power turbine blade

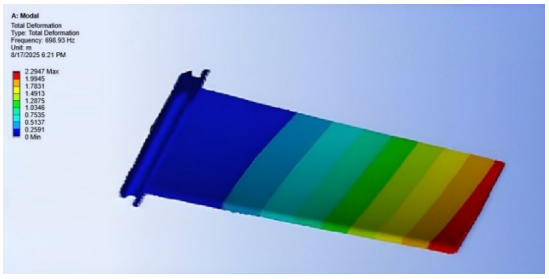

Figure 5: First bending mode shape

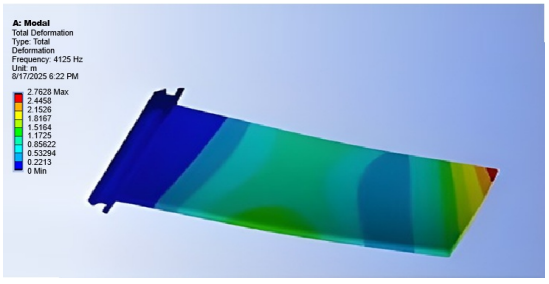

Figure 6: Second bending mode shape

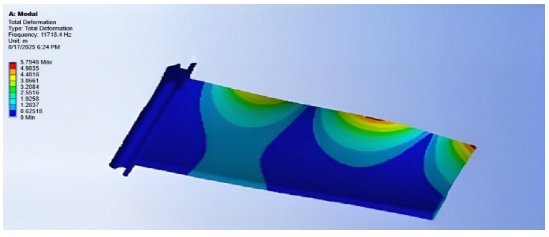

Figure 7: Third bending mode shape

in the high-pressure region of an aircraft power turbine and find the natural frequency as plotted in Figure 8, Figure 9, and Figure 10.

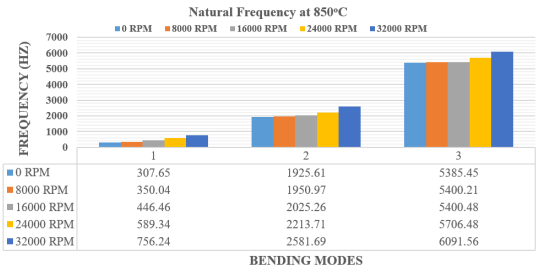

Figure 8: Modal frequency of Titanium Alloy - Ti6Al4V at 850°C with various RPM

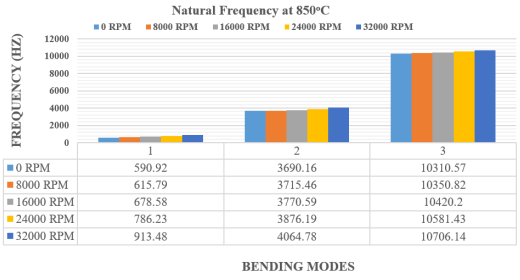

Figure 9: Modal frequency of Inconel-738 at 850°C with various RPM

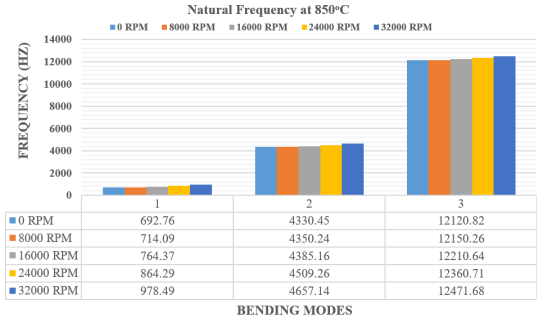

Figure 10: Modal frequency of CM-247 LC at 850°C with various RPM

And the simulation result considering static condition at room temperature is shown in Table 4 below.

4. Result and discussion

4.1. Comparative table of analytical and simulation results at different operating conditions

The comparative analysis between the analytical predictions and ANSYS modal analysis in Table 5 demonstrates strong agreement across all three materials. The analytical model, incorporating centrifugal stiffening effects, accurately captures the trend of increasing natural frequencies with rising rotational speed.

4.2. Material-dependent behavior

- **Titanium Alloy - Ti6Al4V** exhibits the lowest natural frequencies and significant sensitivity to temperature. As both temperature and RPM increase, its stiffness decreases more sharply, leading to low-frequency modes and higher susceptibility to resonance.
- **Inconel-738** maintains higher frequencies and shows relatively small deviations between analytical and FEA results (<2.5%).
- **CM-247 LC** demonstrates the best overall performance, with minimal deviation from analytical predictions (<2%) and consistently high natural frequencies across the RPM range.

4.3. Campbell diagram

Campbell diagrams are prepared on the basis of ANSYS results, which are as shown below.

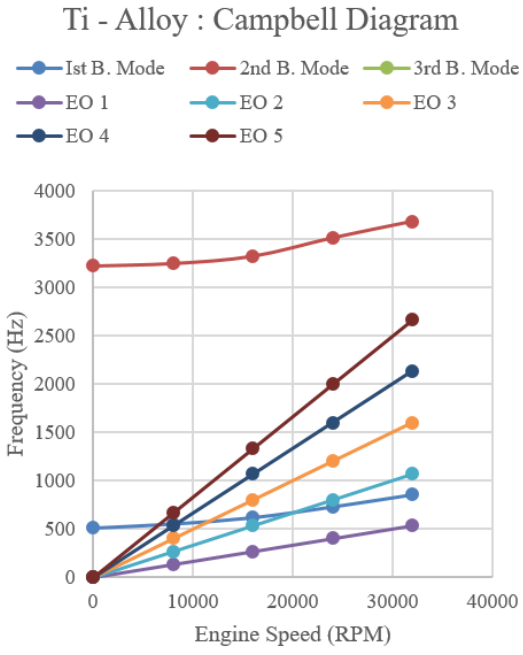

Figure 11: Campbell diagram of Ti – Alloy

Figure 11, Figure 12, and Figure 13 are the Campbell diagrams, which shows the change in natural frequencies of the blade with increase in rotational speed. The intersections between the engine order lines and the modal lines of each material (Ti-6Al-4V, Inconel-738, and CM-247) in camp bell diagrams indicate possible

Table 4: Simulation result considering no rotation and at room temperature

Mode No.	Material	FEA Frequency (Hz)
1	Titanium Alloy - Ti6Al4V	698.93
1	Inconel-738	684.69
1	CM-247 LC (Nickel Alloy)	699.92
3	Titanium Alloy - Ti6Al4V	4125
3	Inconel-738	4092.3
3	CM-247 LC (Nickel Alloy)	4201.2
6	Titanium Alloy - Ti6Al4V	11718.4
6	Inconel-738	11749.6
6	CM-247 LC (Nickel Alloy)	11998.3

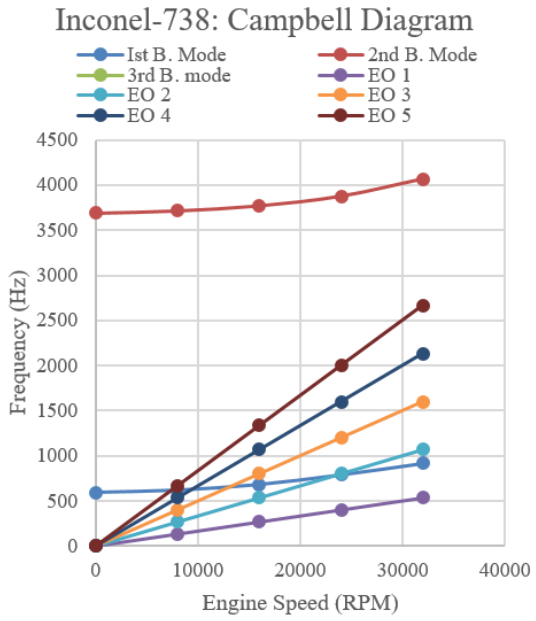

Figure 12: Campbell diagram of Inconel-738

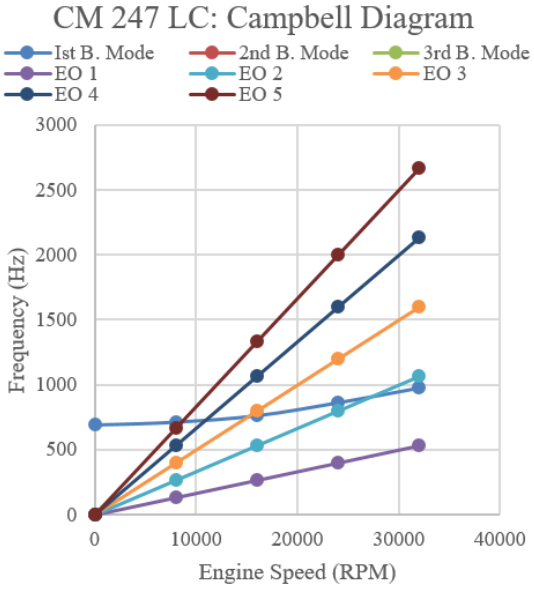

Figure 13: Campbell diagram of CM 247 LC

resonance points. Analysis is mainly done in engine's normal operating range which is taken between 20,000 and 25,000 rpm.

For Ti-6Al-4V, the first bending mode intersects the second engine order line between about 22,000 and 24,000 rpm. This falls within the normal operating range, meaning resonance could occur during regular operation. Whereas, Inconel-738 performs better. Its resonance point shifts to a higher speed range, around 24,000 to 26,000 rpm, slightly above typical cruising speeds. This reduces the likelihood of resonance during normal operation.

The best performance is shown by CM-247. It has the highest natural frequencies, and its resonance crossings occur above 26,000 to 27,000 rpm, which is beyond the engine's usual operating range. This significantly lowers the risk of resonance. Its high stiffness and strong resistance to high temperatures improve durability and operational safety.

5. Conclusion

In this study, an analytical model was first developed to estimate the natural frequencies of the power turbine blade. The blade frequencies were then calculated for both non-operating and operating conditions. After that, finite element modal analysis was carried out in ANSYS to obtain more realistic frequencies and mode shapes. The comparison between analytical and FEA results for the first three bending modes showed good agreement, which confirms that the analytical model is reliable for preliminary design.

Table 5: Comparison of analytical and simulation result at operating conditions

Material	RPM	Bending Mode	Analytical Frequency (Hz)	ANSYS Frequency (Hz)	Error (%)
Titanium Alloy - Ti6Al4V	0	1	523.54	507.65	3.13
		2	3281.15	3225.61	1.72
		3	9188.24	8985.45	2.26
	8000	1	552.58	550.04	0.46
		2	3310.87	3250.97	1.84
		3	9218.05	9024.21	2.15
	16000	1	631.73	616.46	2.48
		2	3398.48	3325.26	2.20
		3	9306.91	9176.48	1.42
	24000	1	745.19	729.34	2.17
		2	3539.54	3513.71	0.74
		3	9453.17	9176.48	3.02
	32000	1	879.79	856.24	2.75
		2	3728.26	3681.69	1.26
		3	9653.77	9431.56	2.36
Inconel-738	0	1	599.41	590.92	1.44
		2	3756.65	3690.16	1.80
		3	10519.78	10310.57	2.03
	8000	1	624.94	615.79	1.49
		2	3782.67	3715.46	1.81
		3	10545.84	10350.82	1.88
	16000	1	695.91	678.58	2.55
		2	3859.49	3770.59	2.36
		3	10623.42	10420.20	1.95
	24000	1	800.39	786.23	1.80
		2	3984.53	3876.19	2.80
		3	10751.81	10581.43	1.61
	32000	1	927.053	913.48	1.49
		2	4152.75	4064.78	2.16
		3	10928.93	10706.14	2.08
CM-247 LC	0	1	703.26	692.76	1.52
		2	4407.50	4330.45	1.78
		3	12342.37	12120.82	1.83
	8000	1	725.14	714.09	1.55
		2	4429.48	4350.24	1.82
		3	12364.56	12150.26	1.76
	16000	1	787.12	764.37	2.98
		2	4495.43	4385.16	2.51
		3	12430.91	12210.64	1.80
	24000	1	880.901	864.29	1.92
		2	4603.04	4509.26	2.08
		3	12540.72	12360.71	1.46
	32000	1	997.27	978.49	1.92
		2	4749.06	4657.14	1.97
		3	12692.85	12471.68	1.77

Using Campbell diagrams, the resonance-sensitive regions are identified by observing the intersection between engine order lines and the modal frequency lines. From this analysis, it is clear that material properties strongly influence resonance behavior.

Among the three materials studied (Ti-6Al-4V, Inconel-738, and CM-247), Ti-6Al-4V shows resonance within the normal operating speed range, making it less suitable for turbine blade applications. Inconel-738 performs better, as its resonance occurs closer to or slightly above the normal operating range. CM-247 shows the safest behavior, with resonance points occurring beyond the engine's typical working speeds.

Therefore, based on natural frequency evaluation, reso-

nance identification, and material comparison, CM-247 is identified as the most suitable material as it avoids resonance within the operating range and maintains strength at elevated temperatures, making it the safest and most reliable option for the power turbine blade, followed by Inconel-738, while Ti-6Al-4V is the least suitable among the three.

6. Recommendation and future work

Based on this study, CM-247 LC is recommended for aircraft power turbine blade applications due to its wider resonance-free operating range under high temperature and rotational speed conditions. Designers should incorporate resonance safety mapping, along with mechanical and thermal properties, during the material selection stage to improve blade reliability and reduce the risk of high-cycle fatigue failure.

Future research may include the incorporation of aerodynamic damping, creep effects at elevated temperatures, and experimental validation of the numerical findings as it is known that creep-induced stiffness reduction and fatigue damage accumulation may lead to gradual changes in natural frequencies during prolonged operation, potentially shifting resonance locations over the blade's service life. More advanced analytical models, such as Timoshenko beam theory, and the consideration of realistic twisted and tapered blade geometries could also be employed to obtain more accurate natural frequency predictions. Additionally, extending the analysis to a full rotor blade assembly with harmonic analysis would provide a more comprehensive understanding of vibration behavior in aircraft turbo engines.

Acknowledgement

No funding and extra assistance was received from any organization for this study.

Conflict of interest

It is declared that there is no any conflict of interest that influence the research or its interpretation.

References

[1] Sadıkoğlu U. Development of aero-thermodynamic cycle design code for turboshaft engines and investigation of fouling effects on performance[D]. Graduate School of Natural and Applied Sciences, 2022.
[2] AZoM. AZo materials – material properties[EB/OL]. 2026. https://www.azom.com/properties.aspx?ArticleID=1547.
[3] Nickel Institute. Alloy IN-738 technical data: A practical guide to the use of nickel-containing alloys[R]. INCO, 1981.
[4] Muñoz-Moreno R, et al. Effect of heat treatment on the microstructure, texture and elastic anisotropy of the nickel-based superalloy CM247LC processed by selective laser melting[J]. Materials Science & Engineering A, 2016.
[5] Moneta G, Out J J. Influence of manufacturing tolerances on vibration frequencies of turbine blade[J]. Machine Dynamics Research, 2014, 38: 105-118.
[6] Herrig L J, Emery J C, Erwin J R. Systematic two-dimensional cascade tests of NACA 65-series compressor blades[R]. National Advisory Committee for Aeronautics (NACA), 1951.
[7] The Engineering Team. Aspect ratio of turbine blade and its significance[Z]. 2021.
[8] Zhang L W, Zheng L, Zhang L Y. Aerodynamic optimization of turbine blade cascade using CFD[J]. Journal of Turbomachinery, 2010, 132(4): 041020-1-041020-8.
[9] Chen J L, Xu X, Chen X J. Effect of trailing-edge thickness on turbine blade performance[J]. ASME Journal of Turbomachinery, 2004, 126(3): 356-362.
[10] Bunker R S. Axial turbine blade aerodynamic design[J]. Journal of Propulsion and Power, 2000, 16(4): 563-571.
[11] Rolls-Royce plc. The jet engine[M]. Rolls-Royce plc, 2015.
[12] cristian. Rolls-Royce Turbomeca RTM322[EB/OL]. 2026. https://www.scribd.com/document/710402333/Rolls-Royce-Turbomeca-RTM322-Wikipedia.
[13] DBpedia Community. Rolls-Royce Turbomeca RTM322[EB/OL]. https://dbpedia.org/page/Rolls-Royce_Turbomeca_RTM322.
[14] Kundrapu R. Turbo presentation[EB/OL]. 2014. https://www.slideshare.net/slideshow/turbo-17121766/17121766.
[15] Saravanamuttoo H I H, Rogers G F C, Cohen H, et al. Gas turbine theory[M]. Pearson Education, 2017.
[16] Gao H, Bai G. Reliability analysis on resonance for low-pressure compressor rotor blade[J]. Advances in Mechanical Engineering, 2015.
[17] Rao S S. Mechanical vibrations[M]. Addison-Wesley, 1995.
[18] Inoyama D. Applicability of Euler–Bernoulli beam theory to thick beams[J]. Journal of Sound and Vibration, 2003.
[19] Rao S S. Mechanical vibrations[M]. Pearson Education, 2017.
[20] Blevins R D. Natural frequency and mode shape[M]. John Wiley & Sons, 2016.
[21] Yang X, et al. A physically-based structure-property model for additively manufactured Ti-6Al-4V[J]. Materials & Design, 2021, 208.
[22] Seif M, et al. Temperature-dependent material modeling for structural steels: Formulation and application[R]. National Institute of Standards and Technology, 2016.
[23] Gowda B C. Tensile properties of SA516, grade 55 steel in the temperature range[C]// ASME/CSME Montreal Pressure Vessel & Piping Conference. 1978: 145-158.